



<b>Title</b>	<b>Quantitative analysis of fiber tractography in cervical spondylotic myelopathy</b>
<b>Author(s)</b>	<b>Wen, Chunyi; Cui, Jiaolong; Lee, Manpan; Mak, Kincheung; Luk, KeithDK; Hu, Yong</b>
<b>Citation</b>	<b>Spine Journal, 2013, v. 13, n. 6, p. 697-705</b>
<b>Issued Date</b>	<b>2013</b>
<b>URL</b>	<b><a href="http://hdl.handle.net/10722/205716">http://hdl.handle.net/10722/205716</a></b>
<b>Rights</b>	<b>NOTICE: this is the author's version of a work that was accepted for publication in The Spine Journal. Changes resulting from the publishing process, such as peer review, editing, corrections, structural formatting, and other quality control mechanisms may not be reflected in this document. Changes may have been made to this work since it was submitted for publication. A definitive version was subsequently published in The Spine Journal, 2013, v. 13 n. 6, p. 697-705. DOI: 10.1016/j.spinee.2013.02.061</b>

1 **Title:** Quantitative Analysis of Fiber Tractography in Cervical Spondylotic Myelopathy

2 **Running Title:** Fiber Tractography and CSM

3

4 Chun-Yi Wen <sup>#</sup>, Jiao-Long Cui <sup>#</sup>, Lee Man Pan, Kin-Cheung Mak, and Keith Dip-Kei. Luk,

5 Yong Hu <sup>\*</sup>

6

7 Department of Orthopaedics and Traumatology, Li Ka Shing Faculty of Medicine, The

8 University of Hong Kong

9

10 “<sup>#</sup>” Equally contribution to this manuscript

11 “<sup>\*</sup>” Corresponding Author

12 Dr. Yong Hu

13 Dept. of Orthopaedics and Traumatology,

14 The University of Hong Kong

15 Address: 12 Sandy Bay Road, Pokfulam, Hong Kong

16 Email address [yhud@hku.hk](mailto:yhud@hku.hk)

17 Tel: (852) 29740336; Fax: (852) 29740335

18

19 **Acknowledgements**

20 The authors would like to thank the support from the General Research Fund from The

21 University Grant Council of Hong Kong (771608M/774211M). The authors would like to

22 thank Prof EX Wu, Drs. Henry Mak and Q Chan for their assistant in MRI scanning.

23

24 **Abstract**

25 **BACKGROUND AND CONTEXT:** Diffusion tensor fiber tractography is an emerging tool  
26 for visualization of spinal cord microstructure. However, there are few quantitative analyses  
27 of the damage in the nerve fiber tracts of the myelopathic spinal cord.

28 **PURPOSE** The aim of this study was to develop a quantitative approach for fiber  
29 tractography analysis in cervical spondylotic myelopathy (CSM).

30 **STUDY DESIGN/SETTING:** Prospective study on a series patients.

31 **MATERIALS AND METHODS** A total of 22 volunteers were recruited with informed  
32 consent, including 15 healthy subjects and 7 CSM patients. The clinical severity of CSM was  
33 evaluated using modified JOA score. The microstructure of myelopathic cervical cord were  
34 analyzed using diffusion tensor imaging (DTI). DTI was performed with a 3.0-Tesla MRI  
35 scanner using pulsed gradient, spin-echo-echo-planar imaging (SE-EPI) sequence. Fiber  
36 tractography was generated via TrackVis with fractional anisotropy threshold set at 0.2 and  
37 angle threshold at 40 degree. Region of interest (ROI) was defined to cover C4 level only or  
38 the whole-length cervical spinal cord from C1 to C7 for analysis. The length and density of  
39 tracked nerve bundles were measured for comparison between healthy subjects and CSM  
40 patients.

41 **RESULTS** The length of tracked nerve bundles significantly shortened in CSM patients as  
42 compared with healthy subjects (healthy: 6.85-77.90 mm; CSM: 0.68-62.53 mm). The density  
43 of the tracked nerve bundles was also lower in CSM patients (healthy:  $0.86 \pm 0.03$ , CSM:  $0.80 \pm$

## Fiber tracking and CSM

44 0.06,  $p < 0.05$ ). Although the definition of ROI covering C4 only or whole cervical cord  
45 appeared not to affect the trend of the disparity between healthy and myelopathic cervical  
46 cords, the density of the tracked nerve bundle through whole myelopathic cords was in an  
47 association with the modified JOA score in CSM cases ( $r = 0.949$ ,  $p = 0.015$ ), yet not found  
48 with ROI at C4 only ( $r = 0.316$ ,  $p = 0.684$ ).

49 **CONCLUSION** The quantitative analysis of fiber tractography is a reliable approach to  
50 detect cervical spondylotic myelopathic lesions compared to healthy spinal cords. It could be  
51 employed to delineate the severity of CSM.

52 **Key words:** Diffusion tensor imaging, Fiber tractography, Cervical spondylotic myelopathy,  
53 Spinal cord.

54

### 55 **Introduction**

56       Cervical spondylotic myelopathy (CSM) is the most common type of spinal cord  
57 dysfunction in patients older than 55 years [1-3]. However, the exact pathophysiology of  
58 CSM remains poorly understood. The natural history of CSM is known to be associated with  
59 the enclosure of the spinal cord in a narrowed canal as a result of degenerative disc and  
60 spondylosis [4]. Nevertheless, the severity of the spinal cord compression does not necessarily  
61 correlate with the signs and symptoms of CSM patients [5-7]. For example, cases with  
62 significant cord compression may not exhibit any neurological signs, while cases with mild  
63 compression of the cord may develop neurological signs [4, 8]. Thus, the changes in gross  
64 morphology of the spinal cord as revealed by anatomical magnetic resonance imaging  
65 (T1-weighted or T2-weighted images) may not reflect the exact pathophysiological changes in  
66 spinal cord [4].

67       There is growing interest in the use of diffusion tensor imaging (DTI) and fiber  
68 tractography (FT) as imaging tools for evaluation of the microstructural changes in spinal  
69 cord trauma and degeneration [9-20]. All such studies have reported a decrease in fractional  
70 anisotropy (FA) of injured or degenerated spinal cord. FA is a commonly used parameter  
71 derived from the eigenvalues of the diffusion matrix [21]; however, eigenvector data have not  
72 been reported. As the principal eigenvector tends to be parallel with the orientation of white  
73 matter fiber bundles, fiber tractography can be generated through integration of  
74 three-dimensional white matter trajectories based on the principal diffusion directions [22].

75 The advantage of fiber tractography is that it provides integrated eigenvalue and eigenvector  
76 data of the diffusion matrix. Several studies [14, 18] have applied visual assessment of FT and  
77 proposed its prognostic value in CSM. However, it is mainly used as a visualization tool for  
78 evaluation of spinal cord lesions [18, 23-26].

79 In validation experiments, microstructural data from fiber tractography images were  
80 compared with histological details [27], providing a foundation for the potential clinical  
81 application of quantitative FT analysis of the spinal cord. Quantitative FT analysis was  
82 recently performed in an attempt to correlate with clinical findings in patients with acute  
83 spinal cord injury [28]. However, to our knowledge there are no studies examining  
84 quantitative FT analysis in CSM, a chronically compressive spinal cord injury.

85 Recently, the quantitative FT analysis was proposed to evaluate chronic compressive  
86 spinal cord lesion, i.e. CSM [18, 19]. There was no agreement yet on the selection of ROI and  
87 morphometric parameters in the quantitative FT analyses for CSM patients. As previous  
88 reported, the maximal compression level (MCL) at Sagittal T2 images of myelopathic cord  
89 was chosen as ROI, while C2 as a reference [19]. The ratio of tracked nerve bundles at MCL  
90 over C2 was measured to correlate the prognosis of CSM after surgical decompression. In  
91 another study, fiber tractography was performed at the selected level as well as C1 and C7.  
92 Only the pattern of fiber tractography was described to correlate the status of neurological  
93 deficit in CSM patients [18]. In this study, we aimed to (1) develop a quantitative FT analysis

94 approach to delineate myelopathic lesions and to correlate it with clinical severity of CSM,  
95 and then (2) investigate the influence of ROI selection and curvature of cervical cord on the  
96 results of FT analyses.

97

## 98 **Materials and Methods**

### 99 *Subjects*

100 The institutional review board of research ethics approved all experimental procedures in  
101 this study. All volunteers were screened to confirm their eligibility. The inclusion criteria for  
102 healthy subjects were those having intact sensory and motor function evaluated, and negative  
103 Hoffman's sign under physical examination. Subjects having any neurological signs and  
104 symptoms or any past history of neurological injury, disease, or operations were excluded.  
105 CSM patients were recruited in authors' institute. Experienced spine surgeons made a clinical  
106 diagnosis of CSM based on the patient's symptoms and signs, as well as radiological findings.  
107 The neurological deficits of CSM patients were systemically evaluated using the Japanese  
108 Orthopaedic Association (JOA) scoring system. The demographic, clinical, radiological and  
109 electrophysiological characteristics of CSM patients were listed in Table 1, which unveiled  
110 the extent of cervical cord involved and the severity of neurological functional impairment.

111

### 112 *MRI Scanning*

113 All images were taken via a 3.0 Tesla MRI scanner (Philips Achieva, Best, the  
114 Netherlands). Pulse sequence programming was performed prior to scanning to optimize the  
115 image quality. During the acquisition process, the subject was placed in a supine position with  
116 the sense neuro-vascular (SNV) head and neck coil enclosing the cervical region, and was  
117 instructed not to swallow to minimize motion artifacts. The subject was then scanned with

## Fiber tracking and CSM

118 anatomical T1-weighted (T1W) and T2-weighted (T2W) images, as well as by diffusion  
119 tensor images (DTI).

120 Sagittal and axial T1W and T2W images were acquired for each subject. A fast spin echo  
121 (FSE) sequence was employed. For sagittal imaging, the imaging parameters were as follows:  
122 field of view (FOV) = 250×250 mm, slice thickness = 3 mm, slice gap = 0.3 mm, fold-over  
123 direction = Feet/Head (FH), number of excitations (NEX) = 2, resolution = 0.92×1.16×3.0  
124 mm<sup>3</sup> (T1W) and 0.78×1.01×3.0 mm<sup>3</sup> (T2W), recon resolution = 0.49×0.49×3.0 mm<sup>3</sup>, and  
125 time of echo (TE) / time of repetition (TR) = 7.2 / 530 ms (T1W) and 120 / 3314 ms (T2W). A  
126 total of 11 sagittal images covering the whole cervical spinal cord were acquired. For axial  
127 imaging, the imaging parameters were as follow: FOV = 80×80 mm, slice thickness = 7 mm,  
128 slice gap = 2.2 mm, fold-over direction = anterior/posterior (AP), NEX = 3, resolution =  
129 0.63×0.68×7.0 mm<sup>3</sup> (T1W) and 0.63×0.67×7.0 mm<sup>3</sup> (T2W), recon resolution =  
130 0.56×0.55×3.0 mm<sup>3</sup> (T1W) and 0.63×0.63×7.0 mm<sup>3</sup> (T2W), and TE / TR = 8 / 1000 ms (T1W)  
131 and 120 / 4000 ms (T2W). Cardiac vectorcardiogram (VCG) triggering was applied to  
132 minimize the pulsation artifact from CSF.

133 A total of 12 axial images covering the whole cervical spinal cord from C1 to C7 were  
134 acquired. Diffusion MRI images were acquired using pulsed sequences: single-shot spin-echo  
135 echo-planar imaging (SE-EPI). Diffusion encoding was in 15 non-collinear and non-coplanar  
136 diffusion directions with a b-value = 600 s/mm<sup>2</sup>. The imaging parameters were as follows:  
137 FOV = 80×80 mm, slice thickness = 7 mm, slice gap = 2.2 mm, fold-over direction = AP,  
138 NEX = 3, resolution = 1.00×1.26×7.0 mm<sup>3</sup>, recon resolution = 0.63×0.64×7.0 mm<sup>3</sup>, and TE /  
139 TR = 60 ms / 5 heartbeats. The image slice planning was the same as the anatomical axial  
140 T1W and T2W images, with 12 slices covering the cervical spinal cord from C1 to C7. The  
141 average duration of diffusion tensor imaging (DTI) was 24 min per subject, with an average  
142 heart rate of 60 beats per min. Spatial saturation with Spectral Presaturation with Inversion  
143 Recovery (SPIR) was applied to suppress the fold-over effect. To alleviate the EPI distortion



144 problem caused by increased magnetic susceptibility at 3.0 T, the distortion correction method  
145 based on the reversed gradient polarity and parallel imaging was employed [29-31].

146

### 147 *Post-processing of Diffusion Tensor Fiber Tractography*

148 Fiber tractography was generated via Diffusion Toolkit v0.6 with interpolated streamline  
149 algorithm and visualized using TrackVis v 0.6 ([www.trackvis.org](http://www.trackvis.org), Harvard Medical School,  
150 Boston, MA, USA). The threshold for fiber tracking termination was set at a voxel with the  
151 fractional anisotropy value lower than 0.20 and/or the angle of principal eigenvectors larger  
152 than 40 degree. The region of interests (ROIs) was defined to cover the whole length of the  
153 cervical spinal cord from C1 to C7 or C4 only (Fig.1.). The ROIs were drawn manually to  
154 cover whole spinal cord with the reference to the b0 image [32]. The track and voxel count,  
155 and the length of tracked fiber in ROIs were automatically calculated via the built-in program  
156 of TrackVis. The density of tracked fibers was calculated as the ratio of the track over the  
157 voxel count in the ROIs. The length of the tracked fiber indicated the fiber connectivity.  
158 Fractional anisotropy (FA) and the trace values (sum of diffusivities) of healthy and  
159 myelopathic spinal cord were also measured accordingly [32, 33].

160

### 161 *Measurement of Spine Cord Curvature*

162 The measurement of spinal cord curvature was performed on T2W sagittal images using  
163 Image J (National Institute of Health, Bethesda, MD, USA). A total of seven lines were drawn  
164 parallel to the intervertebral discs from C1/2 to C7/T1. The angles formed between the line at  
165 C4/5 and the other disc levels were measured, and the summation of the angles showed the  
166 curvature of the cervical spine column as an indicator of spinal cord curvature (Fig. 2). The  
167 healthy spinal cords were categorized as straight (HS) or curved (HC) based on their  
168 curvature below or above the average angle.

169

170 *Statistical Analysis*

171 Comparisons of FA, trace, the track or voxel count, fiber density, and fiber length were  
 172 performed between healthy and CSM patients using the student *t* test. The Spearman  
 173 correlation was conducted to analyze the link between clinical and DTI findings. Further  
 174 analyses were performed after classification by healthy spinal cord curvature using one-way  
 175 ANOVA and *post-hoc* test. The level of significance was set at  $p < 0.05$ . All data analyses were  
 176 performed using SPSS 15.0 analysis software (SPSS Inc, Chicago, IL, USA).

177

178 **Results**

179 A total of 22 volunteers, including 15 adult healthy subjects ( $42 \pm 6$  years old) and 7 CSM  
 180 patients ( $56 \pm 10$  years old), met with the inclusive criteria and were recruited in this study. As  
 181 well as presenting with lower JOA scores (CSM:  $10 \pm 2$  vs full score: 17), CSM patients  
 182 showed a decrease in FA (healthy:  $0.67 \pm 0.08$  vs. CSM:  $0.56 \pm 0.10$ ) and an increase trace  
 183 values (sum of diffusivities) (healthy:  $3.21 \pm 0.22 \times 10^{-3}$  vs. CSM:  $4.42 \pm 1.15 \times 10^{-3}$ ). Fiber  
 184 tractography also revealed that the tracked fibers were loosely organized in myelopathic  
 185 spinal cords, with short or disoriented fibers (Fig. 3), when compared to normal spinal cords.

186

187 *Influence of ROI definition on parameters of quantitative fiber tractography*

188 For both the healthy and the CSM groups, the track count and voxel count in fiber  
 189 tractography were significantly higher when the ROI was set C1 to C7 as compared with the  
 190 ROI at C4 only (Track Count – healthy: C4  $1187.40 \pm 442.06$  vs. C1-C7  $3064.40 \pm 482.38$ ;  
 191 CSM: C4  $367.43 \pm 125.32$  vs. C1-C7  $2282.71 \pm 293.80$ ; Voxel Count – healthy: C4  
 192  $1727.47 \pm 521.81$  vs. C1-C7  $3564.33 \pm 526.65$ ; CSM: C4  $702.57 \pm 232.43$  vs. C1-C7  
 193  $2860.71 \pm 487.76$ ). Further, there was a significant difference in both track and voxel count  
 194 between the healthy and CSM group regardless of ROIs definition at either C1 to C7 or C4  
 195 only (Track Count – C4:  $p = 0.0001$ , C1-C7:  $p = 0.0008$ ; Voxel Count: C4:  $p = 0.0001$ , C1-C7:

196 p=0.0074) (Fig. 4a-b).

197 For both the healthy and the CSM groups, the densities of the tracked fibers were also  
 198 significantly higher when the ROI was set C1 to C7 as compared with the ROI at C4 only  
 199 (healthy: C4  $0.68 \pm 0.07$  vs. C1-C7  $0.86 \pm 0.03$ ; CSM: C4  $0.53 \pm 0.07$  vs. C1-C7  $0.80 \pm 0.06$ ).  
 200 Further, there was a significant difference in the densities of the tracked fibers between the  
 201 healthy and CSM group regardless of ROIs definition at either C1 to C7 or C4 only (C4:  
 202 p=0.0001, C1-C7: p=0.0064) (Fig. 4c).

203 The length of tracked fibers was reduced when changing the ROI from C4 only to the  
 204 whole length of spinal cord (from C1 to C7) (healthy: C4  $43.09 \pm 16.65$  vs. C1-C7  $27.11 \pm 18.33$   
 205 mm; CSM: C4  $25.67 \pm 8.36$  vs. C1-C7  $17.30 \pm 6.06$  mm) (Fig. 4d). The length of fiber track was  
 206 significantly shorter in CSM patients compared with healthy subjects (C4: p=0.0012, C1-C7:  
 207 p=0.0088). The distribution of the length of the tracked fiber is shown in Figure 5. The long  
 208 fiber tracks were obviously lost in CSM (healthy: C4 1.95-76.68 vs. C1-C7 6.85-77.90 mm;  
 209 CSM: 0.68-57.91 vs. C1-C7 0.68-62.53 mm).

210 Although the definition of ROI covering C4 only or whole cervical cord appeared not to  
 211 affect the trend of the disparity between healthy and myelopathic cervical cords, the density of  
 212 the tracked nerve bundle through whole myelopathic cords was in an association with the  
 213 modified JOA score in CSM cases ( $r=0.949$ ,  $p=0.015$ ), yet not found with ROI at C4 only  
 214 ( $r=0.316$ ,  $p=0.684$ ).

215

#### 216 *Influence of spinal cord curvature on parameters of quantitative fiber tractography*

217 There was an obvious difference in the curvature of the cervical spine between  
 218 individuals observed when placing for MRI scanning. The average angle for the curvature of  
 219 the cervical spine was  $20.4^\circ$  in healthy subjects. A total of six healthy subjects had a 'straight'  
 220 spinal cord (HS group), ranging from  $10.1^\circ$  to  $18.5^\circ$ , while nine healthy subjects had a  
 221 'curved' spinal cord (HC), ranging from  $20.4^\circ$  to  $30.4^\circ$ . The mean curvature of myelopathic

222 spinal cord was  $43.6^\circ$ , ranging from  $42.4^\circ$  to  $44.47^\circ$ . In the ROI from C1 to C7, the track and  
223 voxel count was significantly lower in the curved compared with the straight spinal cord  
224 (Track count – HS:  $3236.33 \pm 537.23$  vs. HC:  $2805.38 \pm 813.26$ ; Voxel count – HS:  
225  $3730.17 \pm 525.04$  vs. HC:  $3295.02 \pm 995.32$ ). In comparison with the straight or curved healthy  
226 spinal cord, both track and voxel count were decrease in CSM (Track count: HS vs. CSM,  
227  $p=0.002$ ; HC vs. CSM,  $p=0.003$ ; Voxel count: HS vs. CSM,  $p=0.01$ ; HC vs. CSM,  $p=0.03$ )  
228 (Fig. 6a-b).

229 There was no significant effect of spinal cord curvature on the density and length of the  
230 tracked fibers (HS:  $30.33 \pm 8.69$  vs. HC:  $25.32 \pm 8.77$ ). There was a marginal difference detected  
231 in the density under the sub-group analysis according to the curvature of spinal cord (HS vs.  
232 CM,  $p=0.046$ ; HC vs. CM,  $p=0.054$ ) (Fig. 6c). The length of the fiber track remained lower in  
233 the CSM than in healthy subjects regardless of presence of a straight or curved spinal cord  
234 (HS vs. CSM,  $p=0.001$ ; HC vs. CSM, C1-C7,  $p=0.028$ ) (Fig. 6d).

235

## 236 Discussion and Conclusion

237 Cervical spondylotic myelopathy is a clinical diagnosis based on the description of a  
238 chronic compression of spinal cord in a stenotic canal as a result of spondylosis and/or disc  
239 degeneration with subsequent neurological deficit [1]. However, the wide range of clinical  
240 signs and symptoms and non-specific information of anatomical MRI have made it difficult to  
241 make a precise diagnosis of CSM (e.g., the delineation of the extent or severity of  
242 myelopathic lesion) [1]. In the present study, using diffusion tensor fiber tractography, we  
243 developed a direct quantitative approach to quantify the organization and connectivity of fiber  
244 bundles in the spinal cord in the living human body in a non-invasive manner. We found that  
245 quantitative analysis of fiber tractography (FT) could reliably detect the microstructural  
246 difference between healthy and myelopathic spinal cord, regardless of ROI selection and  
247 spinal cord curvature. Importantly, we used the fiber length parameter to indicate the

248 connectivity of fiber bundles in the spinal cord, which was sensitive for detection of poor  
249 fiber bundle organization in CSM. By contrast, fiber density exhibited poor sensitivity. The  
250 poor fiber organization in CSM was reflected by a decrease in FA and an increase in  
251 diffusivity .

252 Chang Y *et al.* previously examined the number of passing fibers in the spinal cord in  
253 cases of cervical spinal cord trauma using a C4 level ROI [28]. Recently, the quantitative FT  
254 analyses were also employed in CSM cases [18, 19]. However, the selection of ROI and  
255 parameters varied among these studies. The maximal compression level of myelopathic  
256 cervical cord was chosen with C2 as a reference to calculate the ratio of tracks in fiber  
257 tractography [19]. In the other study, the selected level was analyzed with C1 and C7 as the  
258 reference [18]. Importantly, the prognostic value of quantitative FT analyses was implied in  
259 surgical management of CSM patients. It was shown that the ratio or pattern of tracked nerve  
260 fibers appeared to correlate with the postoperative improvement of CSM patients after  
261 surgical decompression. However, they did not examine the influence of ROI selection on the  
262 outcome of the quantitative FT analysis. As shown in the present study, ROI selection can  
263 influence the exact values generated from quantitative FT analysis. For example, the track and  
264 voxel count and the density of tracked fibers were higher when the whole length spinal cord  
265 was selected rather than the C4 level only. Although this did not change the trend of  
266 CSM-related changes, the three-dimensional image of fiber tractography with the C1 to C7  
267 ROI selection was more close to the actual volume and structure of the spinal cord (Fig.1).  
268 Importantly, we found that the density of tracked nerve bundles correlated well with the  
269 clinical severity of CSM when the myelopathic cervical cord from C1 to C7 was analyzed as a  
270 whole. Our findings suggested that the ROI from C1 to C7 should be taken, rather than MCL  
271 only, to reflect the overall status of myelopathic cervical cord.

272 We also explored the influence of the curvature of the spinal cord on FT analysis, and  
273 found that spinal cord curvature did not alter the trend of CSM-related changes. However, the

274 data from subjects with a curved spinal cord exhibited a large variation, and analyses failed to  
275 detect a significant difference in the fiber density between healthy and myelopathic spinal  
276 cord after taking spinal cord curvature into consideration, particularly when choosing C1-7 as  
277 an ROI. Nevertheless, we did detect a statistically significant difference in the parameters of  
278 FT analysis (i.e., length of tracked fibers). A recent report used the fiber tract (FT) ratio as a  
279 quantitative assessment of the spinal cord, and found a significant correlation with the  
280 recovery rates in CSM patients [19]. However, in that study the FT ratio did not reflect the  
281 severity of neurological deficit.

282 We found that the track count (i.e., the number of fiber projections) and the voxel count  
283 (i.e., the number of voxels) that passed through the tracked fibers in the ROIs were  
284 significantly lower in the injured spinal cord as compared with the healthy spinal cord. This  
285 may be explained by reduction in the seed points for fiber bundles from the basic principle of  
286 fiber tractography [34]. As each seed point was screened by the values of FA, the low FA in  
287 CSM indicated loss of anisotropy of the diffusion ellipsoid of water molecules, as previously  
288 reported [9-17]. As such, less water molecules could be used as the seed points for the  
289 subsequent fiber tracking, resulting in loss of track count and track density. The length of the  
290 tracked fibers was statistically different between healthy and diseased groups. Although the  
291 tracking did not originate from the actual anatomical structure of the nerve bundles in the  
292 spinal cord, these data indicate a continuity of intact nerve fibers, as the anisotropy of water  
293 molecules occurs preferentially along the fiber bundle. The longer the fiber tracking, the  
294 better integrity and connectivity of a real nerve bundle. Importantly, all these findings were in  
295 agreement with histopathological findings of CSM, including axon damage and/or  
296 demyelination [35].

297 There are several limitations of our study. First, we used relatively thicker axial slices (7  
298 mm) for diffusion MR imaging when compared with the previous studies (3 or 5 mm). The  
299 gap of 2.2 mm adopted between slices would lead to loss of information during the process of

## Fiber tracking and CSM

300 three-dimensional reconstruction of fiber tractography. Further, we only used a single  
301 orientation for one voxel in fiber tractography, resulting in a potential for incorrect (false  
302 positive) or ineffective tracking (false negative) in voxels with more than one orientation of  
303 fiber bundles. Finally, CSM is a result of age-related degeneration of the cervical spine with  
304 abnormal curvature in elderly persons. However, for the small number of the subjects  
305 recruited in our study, the age of healthy subjects (42 years) was younger than in the patient  
306 group (approximately 56 years). Further, the subjects showed disparity in cervical spine  
307 curvature (HS: 10.1-18.5; HC: 20.4-30.4; CSM: 42.4-44.47). Thus, these potentially  
308 confounding factors should be controlled in a future large-scale population study.

309 In summary, we introduced a reliable quantitative analysis approach for diffusion tensor  
310 fiber tractography to delineate the extent and severity of spinal tract damages in CSM. We  
311 also identified the confounding factors, i.e. ROI selection and curvature of cervical spine,  
312 which could affect the outcome of the quantitative FT analyses for CSM patients.

313

## 314 References

- 315 1. McCormick, W.E., M.P. Steinmetz, and E.C. Benzel, *Cervical spondylotic myelopathy: make the*  
 316 *difficult diagnosis, then refer for surgery.* Cleve Clin J Med, 2003. 70(10): p. 899-904.
- 317 2. Ichihara, K., et al., *Mechanism of the spinal cord injury and the cervical spondylotic myelopathy: new*  
 318 *approach based on the mechanical features of the spinal cord white and gray matter.* J Neurosurg,  
 319 2003. 99(3 Suppl): p. 278-285.
- 320 3. Rao, R., *Neck Pain, Cervical Radiculopathy, and Cervical Myelopathy: Pathophysiology, Natural*  
 321 *History, and Clinical Evaluation.* The Journal of Bone & Joint Surgery, 2002. 84(10): p. 1872-1881.
- 322 4. Baron, E.M. and W.F. Young, *Cervical spondylotic myelopathy: a brief review of its pathophysiology,*  
 323 *clinical course, and diagnosis.* Neurosurgery, 2007. 60(1 Suppl 1): p. S35-41.
- 324 5. Matsumoto, M., et al., *Increased signal intensity of the spinal cord on magnetic resonance images in*  
 325 *cervical compressive myelopathy. Does it predict the outcome of conservative treatment?* Spine (Phila  
 326 Pa 1976), 2000. 25(6): p. 677-82.
- 327 6. Bednarik, J., et al., *Presymptomatic spondylotic cervical myelopathy: an update predictive model.* Eur  
 328 Spine J, 2008. 17: p. 421-431.
- 329 7. Kadanka, Z., et al., *Cross-sectional Transverse Area and Hyperintensities on Magnetic Resonance*  
 330 *Imaging in Relation to the Clinical Picture in Cervical Spondylotic Myelopathy.* Spine, 2007. 32(23): p.  
 331 2573-2577.
- 332 8. Baptiste, D.C. and M.G. Fehlings, *Pathophysiology of cervical myelopathy.* The Spine Journal, 2006.  
 333 6: p. 190S-197S.
- 334 9. Facon, D., et al., *MR Diffusion Tensor Imaging and Fiber Tracking in Spinal Cord Compression.* Am  
 335 J Neuroradiol, 2005. 26: p. 1587-1594.
- 336 10. Demir, A., et al., *Diffusion-weighted MR imaging with apparent diffusion coefficient and apparent*  
 337 *diffusion tensor maps in cervical spondylotic myelopathy.* Radiology, 2003. 229(1): p. 37-43.
- 338 11. Mamata, H., F.A. Jolesz, and S.E. Maier, *Apparent diffusion coefficient and fractional anisotropy in*  
 339 *spinal cord: age and cervical spondylosis-related changes.* J Magn Reson Imaging, 2005. 22(1): p.  
 340 38-43.
- 341 12. Xiangshui, M., et al., *3 T magnetic resonance diffusion tensor imaging and fibre tracking in cervical*  
 342 *myelopathy.* Clin Radiol, 2010. 65(6): p. 465-73.
- 343 13. Chang, Y., et al., *Diffusion Tensor Imaging and Fiber Tractography of Patients with Cervical Spinal*  
 344 *Cord Injury.* J Neurotrauma, 2010.
- 345 14. Budzik, J.F., et al., *Diffusion tensor imaging and fibre tracking in cervical spondylotic myelopathy.*  
 346 Eur Radiol, 2010.
- 347 15. Song, T., et al., *Diffusion tensor imaging in the cervical spinal cord.* Eur Spine J, 2010.
- 348 16. Voss, H.U., et al., *Diffusion Tensor Imaging in Cervical Spondylotic Myelopathy.* World Spine  
 349 Journal, 2007. 2(3): p. 140-147.
- 350 17. Shanmuganathan, K., et al., *Diffusion tensor MR imaging in cervical spine trauma.* AJNR Am J  
 351 Neuroradiol, 2008. 29(4): p. 655-9.



- 352 18. Lee, J.W., et al., *Diffusion tensor imaging and fiber tractography in cervical compressive myelopathy: preliminary results*. *Skeletal Radiol*, 2011. 40(12): p. 1543-51.
- 353
- 354 19. Nakamura, M., et al., *Clinical significance of diffusion tensor tractography as a predictor of functional recovery after laminoplasty in patients with cervical compressive myelopathy*. *J Neurosurg Spine*, 2012. 17(2): p. 147-52.
- 355
- 356
- 357 20. Chang, Y., et al., *Diffusion tensor imaging and fiber tractography of patients with cervical spinal cord injury*. *J Neurotrauma*, 2010. 27(11): p. 2033-40.
- 358
- 359 21. Basser, P.J. and D.K. Jones, *Diffusion-tensor MRI: theory, experimental design and data analysis - a technical review*. *NMR in Biomedicine*, 2002. 15: p. 456-467.
- 360
- 361 22. Mori, S. and P.C. van Zijl, *Fiber tracking: principles and strategies - a technical review*. *NMR in biomedicine*, 2002. 15(7-8): p. 468-80.
- 362
- 363 23. Facon, D., et al., *MR diffusion tensor imaging and fiber tracking in spinal cord compression*. *AJNR. American journal of neuroradiology*, 2005. 26(6): p. 1587-94.
- 364
- 365 24. Xiangshui, M., et al., *3 T magnetic resonance diffusion tensor imaging and fibre tracking in cervical myelopathy*. *Clinical radiology*, 2010. 65(6): p. 465-73.
- 366
- 367 25. Budzik, J.F., et al., *Diffusion tensor imaging and fibre tracking in cervical spondylotic myelopathy*. *European radiology*, 2011. 21(2): p. 426-33.
- 368
- 369 26. Budzik, J.F., et al., *Diffusion tensor imaging and fibre tracking in cervical spondylotic myelopathy*. *Eur Radiol*, 2011. 21(2): p. 426-33.
- 370
- 371 27. Flint, J.J., et al., *Cellular-level diffusion tensor microscopy and fiber tracking in mammalian nervous tissue with direct histological correlation*. *NeuroImage*, 2010. 52(2): p. 556-61.
- 372
- 373 28. Chang, Y., et al., *Diffusion tensor imaging and fiber tractography of patients with cervical spinal cord injury*. *Journal of neurotrauma*, 2010. 27(11): p. 2033-40.
- 374
- 375 29. Morgan, P.S., et al., *Correction of spatial distortion in EPI due to inhomogeneous static magnetic fields using the reversed gradient method*. *J Magn Reson Imaging*, 2004. 19(4): p. 499-507.
- 376
- 377 30. Chuang, T.C., et al., *PROPELLER-EPI with parallel imaging using a circularly symmetric phased-array RF coil at 3.0 T: application to high-resolution diffusion tensor imaging*. *Magn Reson Med*, 2006. 56(6): p. 1352-8.
- 378
- 379
- 380 31. Andersson, J.L., S. Skare, and J. Ashburner, *How to correct susceptibility distortions in spin-echo echo-planar images: application to diffusion tensor imaging*. *NeuroImage*, 2003. 20(2): p. 870-88.
- 381
- 382 32. Cui, J.L., et al., *Entropy-based analysis for diffusion anisotropy mapping of healthy and myelopathic spinal cord*. *Neuroimage*, 2011. 54(3): p. 2125-31.
- 383
- 384 33. Cui, J.L., et al., *Orientation entropy analysis of diffusion tensor in healthy and myelopathic spinal cord*. *Neuroimage*, 2011. 58(4): p. 1028-33.
- 385
- 386 34. Ciccarelli, O., et al., *Spinal cord spectroscopy and diffusion-based tractography to assess acute disability in multiple sclerosis*. *Brain : a journal of neurology*, 2007. 130(Pt 8): p. 2220-31.
- 387
- 388 35. Beaulieu, C., et al., *Changes in water diffusion due to Wallerian degeneration in peripheral nerve*. *Magnetic resonance in medicine : official journal of the Society of Magnetic Resonance in Medicine / Society of Magnetic Resonance in Medicine*, 1996. 36(4): p. 627-31.
- 389
- 390



Figure1  
[Click here to download high resolution image](#)

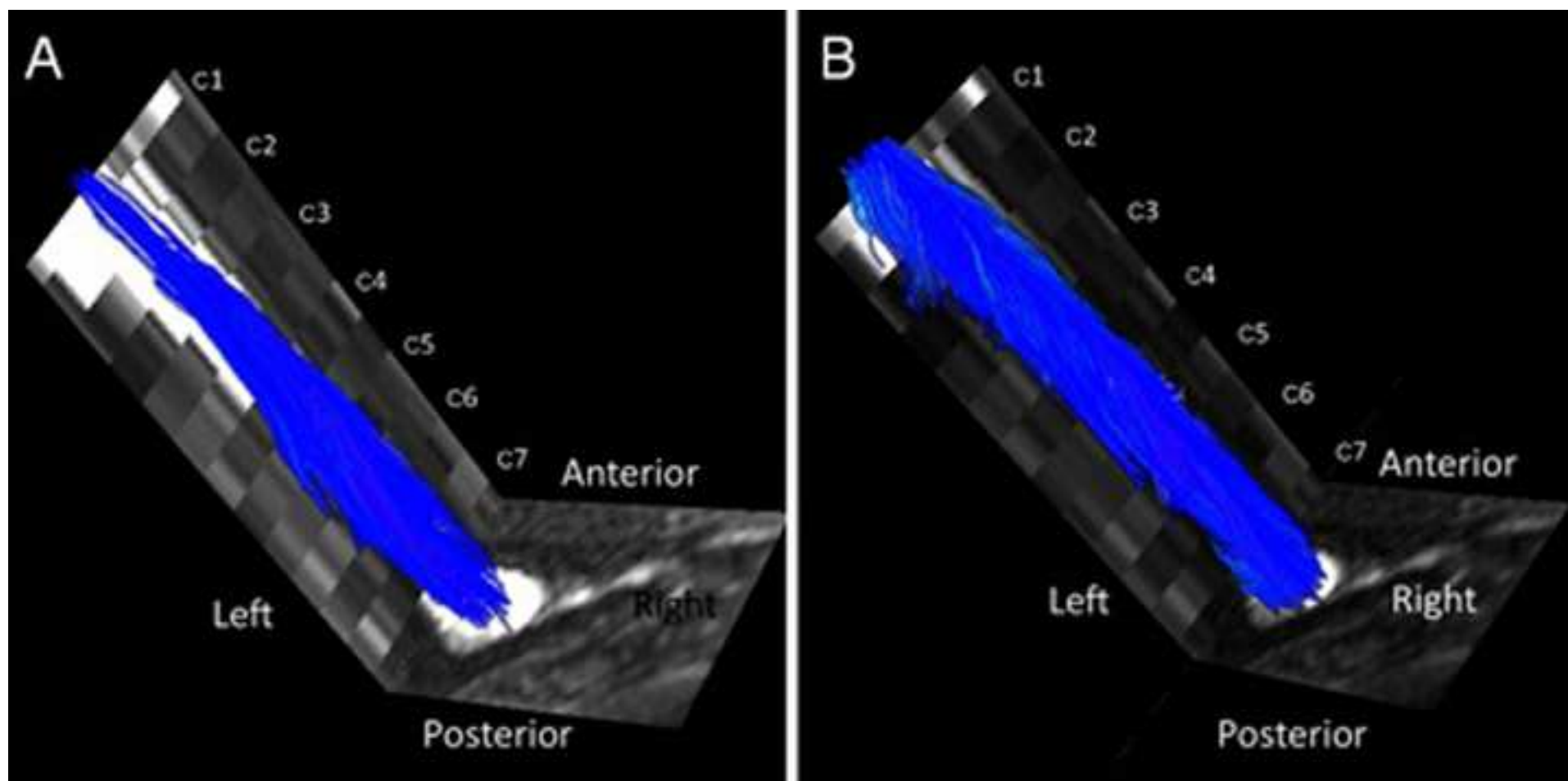


Figure2

[Click here to download high resolution image](#)



Figure3  
[Click here to download high resolution image](#)

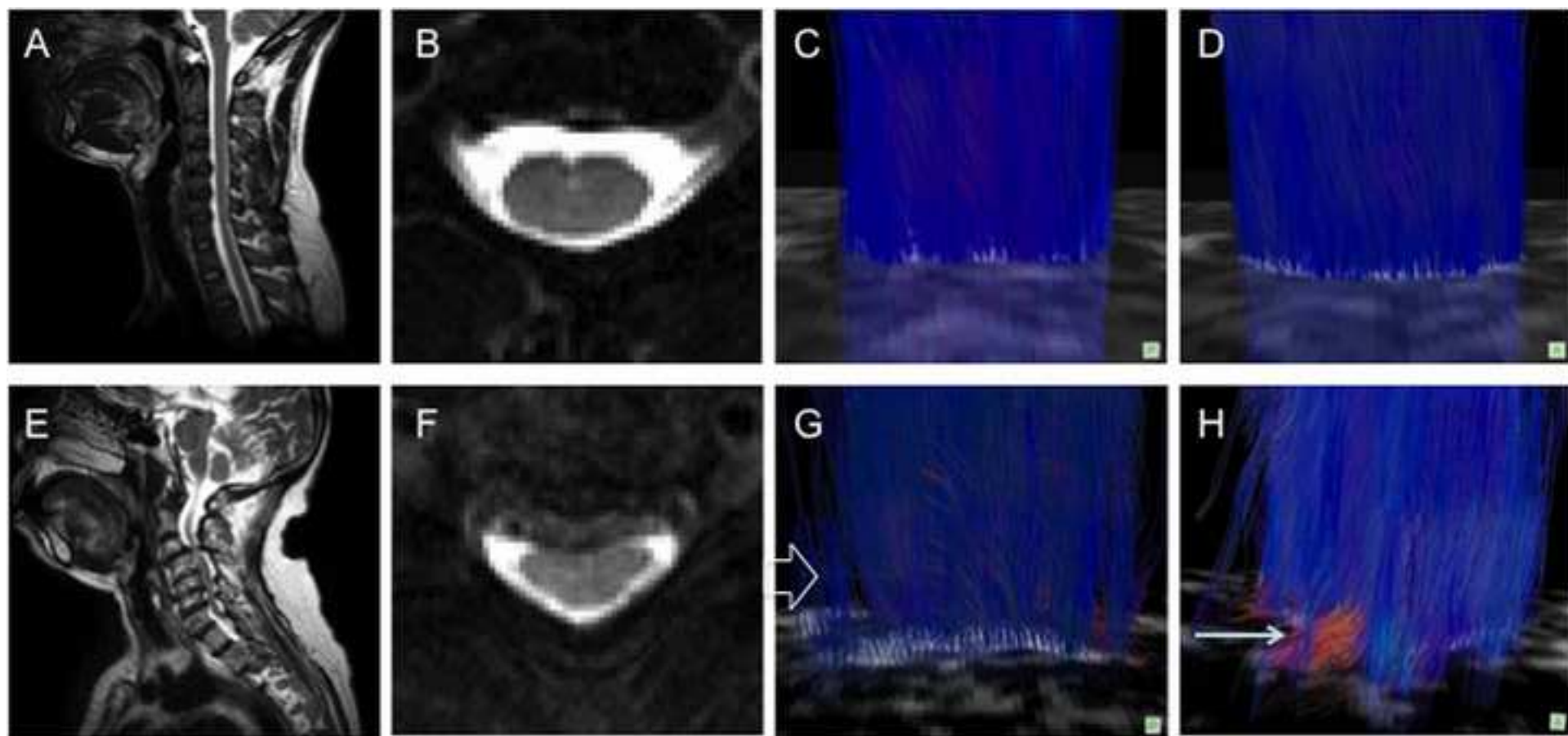


Figure4

[Click here to download high resolution image](#)

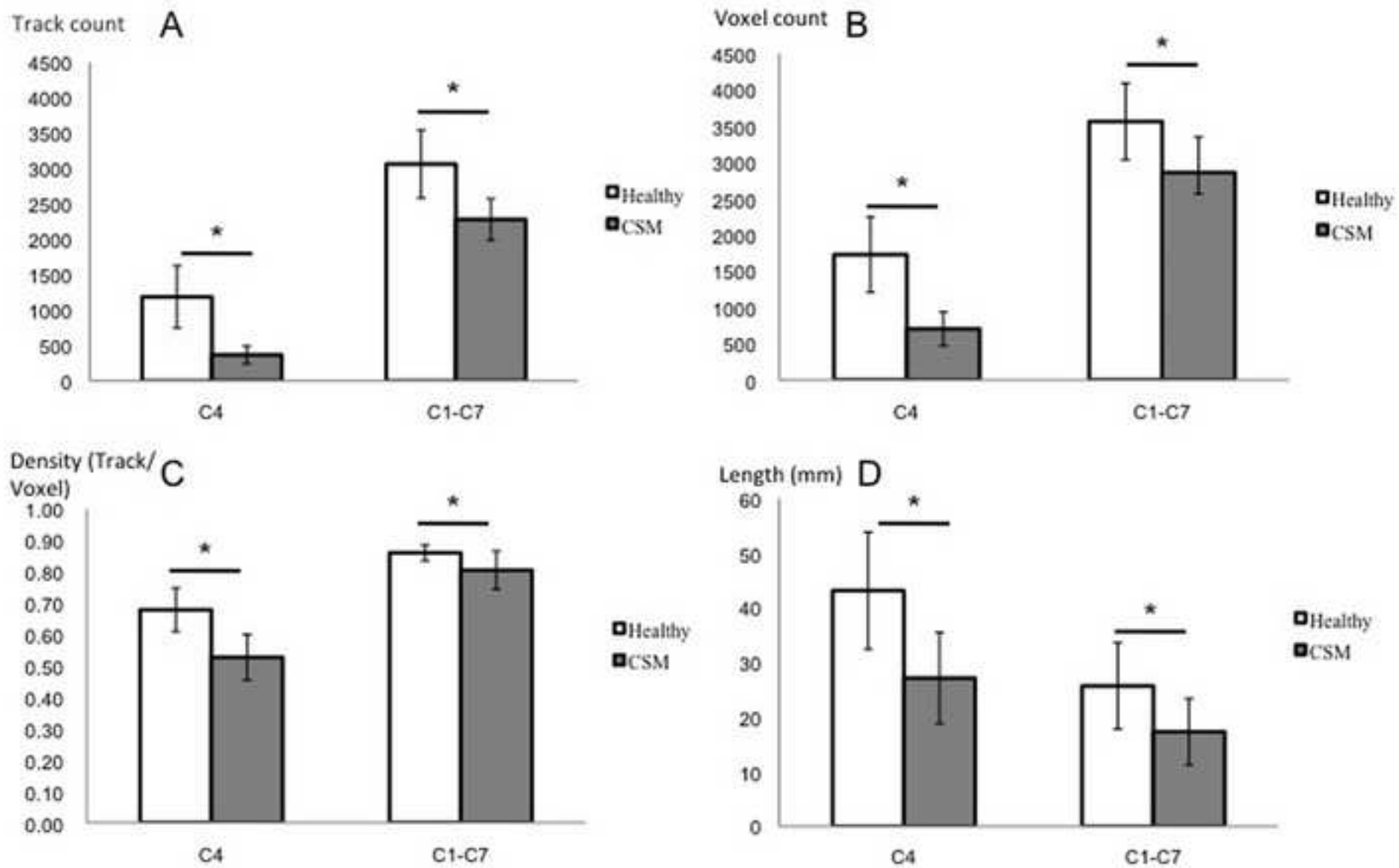


Figure5  
[Click here to download high resolution image](#)

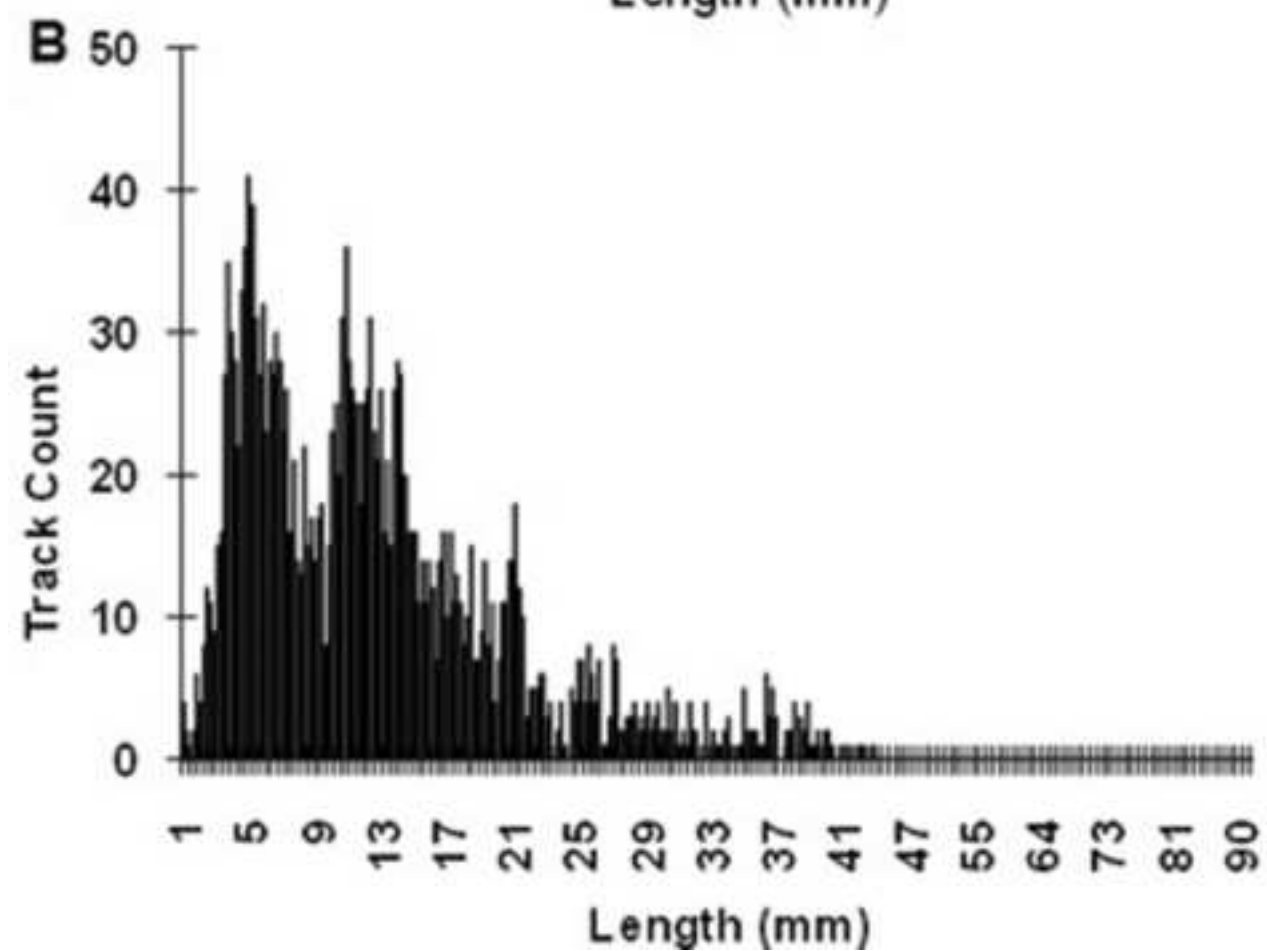
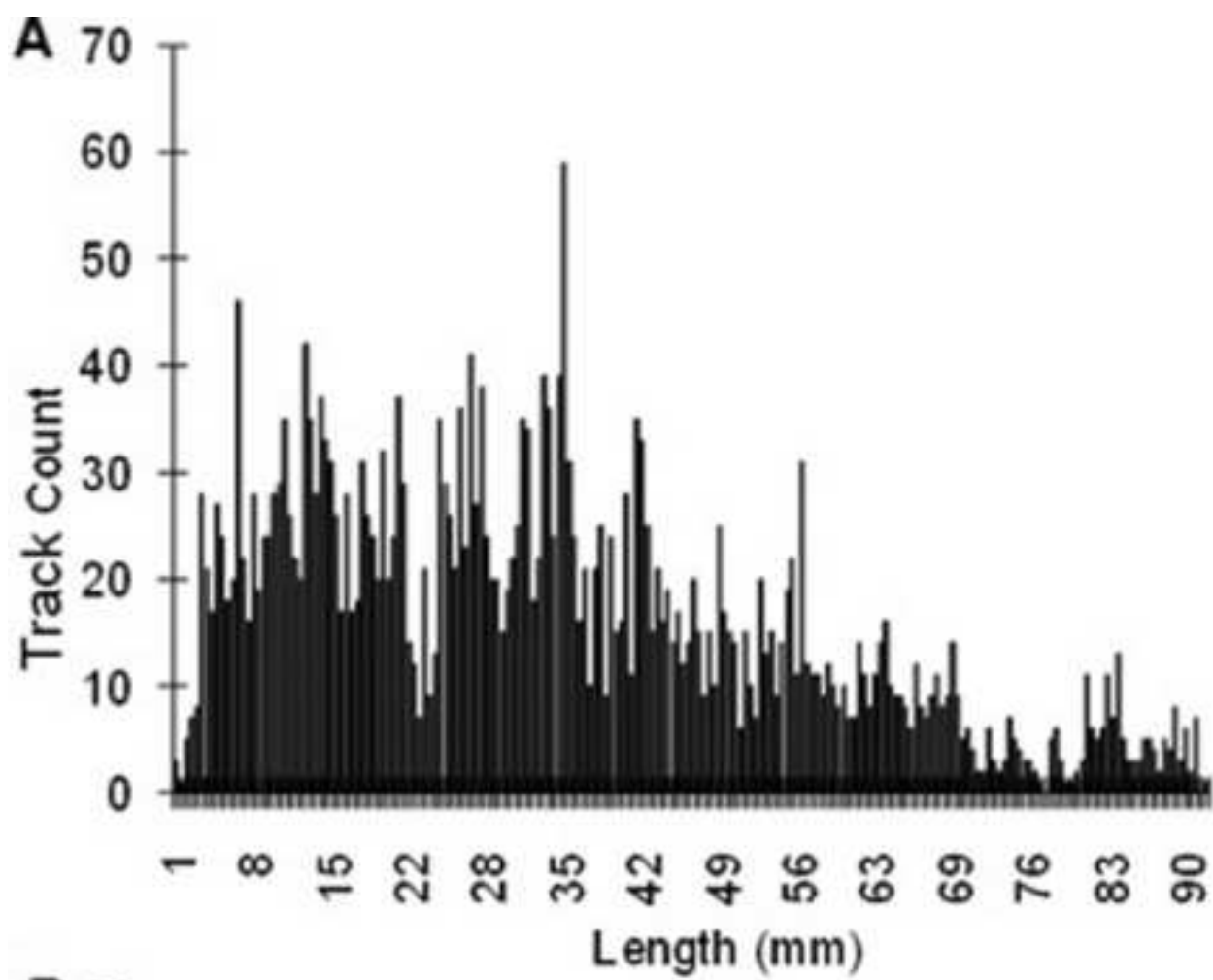


Figure6

[Click here to download high resolution image](#)

